Medical Engineering & Physics 36 (2014) 1041–1046



Medical Engineering & Physics

journal homepage: www.elsevier.com/locate/medengphy

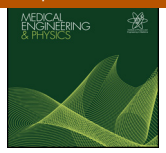

# *In vivo* application of an optical segment tracking approach for bone loading regimes recording in humans: A reliability study

Peng-Fei Yang[a,b,c,*], Maximilian Sanno[c], Bergita Ganse[b], Timmo Koy[d], Gert-Peter Brüggemann[c], Lars Peter Müller[d], Jörn Rittweger[b]

[a] Key Laboratory for Space Bioscience and Biotechnology, School of Life Sciences, Northwestern Polytechnical University, Xi'an, China
[b] Institute of Aerospace Medicine, German Aerospace Center, Cologne, Germany
[c] Institute of Biomechanics and Orthopaedics, German Sport University Cologne, Germany
[d] Department of Orthopaedic and Trauma Surgery, University of Cologne, Germany

ARTICLE INFO

*Article history:*
Received 12 June 2013
Received in revised form 25 April 2014
Accepted 11 May 2014

*Keywords:*
Tibia segment deformation
Optical approach
*In vivo*
Motion capture system
Locomotive activities

ABSTRACT

This paper demonstrates an optical segment tracking (OST) approach for assessing the *in vivo* bone loading regimes in humans. The relative movement between retro-reflective marker clusters affixed to the tibia cortex by bone screws was tracked and expressed as tibia loading regimes in terms of segment deformation. Stable *in vivo* fixation of bone screws was tested by assessing the resonance frequency of the screw-marker structure and the relative marker position changes after hopping and jumping. Tibia deformation was recorded during squatting exercises to demonstrate the reliability of the OST approach. Results indicated that the resonance frequencies remain unchanged prior to and after all exercises. The changes of Cardan angle between marker clusters induced by the exercises were rather minor, maximally 0.06°. The reproducibility of the deformation angles during squatting remained small (0.04°/m–0.65°/m). Most importantly, all surgical and testing procedures were well tolerated. The OST method promises to bring more insights of the mechanical loading acting on bone than in the past.



## 1. Introduction

The loading patterns of bones constitute an important determinant for their current geometry and mechanical properties [1]. Further understanding of the bone loading patterns would improve our comprehension of the mechanical adaptation process of bones [2–4]. Certainly, bone loading patterns can be experimentally assessed in some particular cases. A series of classic animal studies in the 1980s investigated long bone loading patterns using typically three strain gauges attached around the mid-shaft of the bone's surface [5,6]. However, substantial prediction error may be induced using strain gauge approaches [7]. Beyond that, the strain gauge approaches may not be suitable for application in many other species, including humans. Despite its invasiveness, the regular muscle function may be disturbed if strain gauges have to be attached around the bone [7,8]. To our knowledge, the current understanding of long bone loading pattern in humans during activities remains limited due to the technical difficulties.

In our previous publication, we proposed a new concept of optical segment tracking (OST) approach for assessing *in vivo* long bone loading pattern, in terms of segment deformation regimes [9]. The idea was to affix clusters with sets of retro-reflective markers to different sites of the bone, and to track the trajectories of these markers with a motion capture system during different locomotor tasks. Bone segment deformation, *i.e.* bending and torsion, can then be assessed from the relative movement between the markers. Since the OST approach is based on coordinate tracking of the markers, its resolution, accuracy, and repeatability entirely rely on the performance of the adopted optical system. Mock-testing with the optical system has demonstrated that a resolution of <20 μm can be achieved with high accuracy and precision within a volume of 400 mm × 300 mm × 300 mm [9]. High repeatability of the OST approach in recording minute tibia deformations was also demonstrated in a human cadaveric testing (supplementary material). However, whether or not the OST approach is practically feasible in humans still remains to be determined. The general toleration of the test subjects to the OST approach has been reported previously [10]. In this paper, firstly, the stability of bone screws in

* Corresponding author at: Key Laboratory for Space Bioscience and Biotechnology, School of Life Sciences, Northwestern Polytechnical University, Youyi Xilu 127, 710072 Xi'an, China. Tel.: +86 29 88491613; fax: +86 29 88491671.
*E-mail addresses:* yangpf@nwpu.edu.cn, xgdypf@gmail.com (P.-F. Yang).

http://dx.doi.org/10.1016/j.medengphy.2014.05.005
1350-4533/

the tibia throughout several exercises was evaluated using resonance frequency analysis. Secondly, the *in vivo* reliability of the OST approach was demonstrated using the tibia deformation results of a squatting exercise.

## 2. Materials and methods

Five healthy male subjects (26–50 years old) volunteered to participate in the study. The study protocol was approved by the relevant ethics bodies, and written informed consent was obtained from all subjects before inclusion into the study. The operations and the *in vivo* exercise battery were performed at the Department of Orthopedic and Trauma Surgery of the University Hospital of Cologne.

### 2.1. Surgical and bone visualization technique

On the right shank of each subject, surgical implantation and explantation of the bone screws were performed under local anesthesia by injecting Xylocain 1% and Carbostesin 0.5% into the skin and the periosteum. Prior to that, Ibuprofen (600 mg) and Cefuroxime (1500 mg) were administered [10]. Further details regarding the surgical technique have been reported previously [10]. Approximately one week prior to the *in vivo* experiments, transverse MRI (Magnetic Resonance Imaging, sequence: 601, slice thickness/distance: 5/5.5 mm, resolution: 0.27 mm, 1.5 T, Philips, Best, The Netherlands) images of the entire tibia were obtained to select those sites of the tibia where the cortex was at least 4 mm thick for bone screw installation. Eventually, the antero-medial aspect sites of tibia were selected at mid-site of the tibia diaphysis, approximately 10 cm below the tibia plateau and above the medial malleolus, respectively. Surgical incisions of approximately 1 cm length were made (Fig. 1A), and holes were drilled 2–3 mm into the tibia cortex with a 2.1 mm diameter drill (Stryker Leibinger GmbH & Co. KG, Germany) into which the bone screws (Asnis Micro cannulated titanium screws, ⌀3 mm, total/thread length: 24/6 mm, Stryker Leibinger GmbH & Co. KG, Germany) were implanted.

Bone screw removal after the testing took place between 6 and 8 h later. Bone screw positions were documented using 6 scans by peripheral quantitative computed tomography (pQCT) with a XCT 3000 (slice thickness/distance: 2.5/1.5 mm, pixel size: 0.4 mm, Stratec Medizintechnik, Pforzheim, Germany) after screw removal (Fig. 1D).

### 2.2. OST approach

Onto each bone screw, a marker cluster, with a set of three non-collinear, high surface quality retro-reflective markers (⌀5 mm, Géodésie Maintenance Services, Nort Sur Erdre, France) was mounted using tiny screws for fixation (Fig. 1C). A Vicon MX optical motion capture system with eight Vicon F40 cameras (Vicon Motion System Ltd., LA, USA) was used to capture the trajectories of the marker clusters at 300 Hz (Fig. 1B). In order to obtain optimal accuracy and precision, the optical system was configured as previously proposed [9]. Of note, by keeping the full resolution of the cameras (maximum sampling rate with full resolution is 370 Hz), a much higher sampling frequency than in the previously proposed configuration was realized to capture the relatively fast movements of the markers during the *in vivo* experiments. Compared to previous surface tracking approaches that use skin-attached markers, the OST approach totally avoids the potential influence of the relative movement between skin and bone on the recorded results.

### 2.3. Stability of bone screws: resonance frequency

The resonance frequency of the screw-marker structure from two subjects was assessed prior to and after the exercises, including approximately 10 min of walking, 10 min of running, 30 cycles of double legs hopping, 30 cycles of single leg hopping, 3 drop jumps and 3 countermovement jumps. The proximal screw-cluster structure was excited by flipping with a finger of the same lab staff while the subject was in sitting position with the shank free of any loading. The marker trajectories were simultaneous recorded at 1000 Hz.

### 2.4. Stability of bone screws: relative movement between the tibia-affixed markers

The constancy of the relative position between the marker clusters across the repetitions of the most intense exercises, *i.e.* hopping

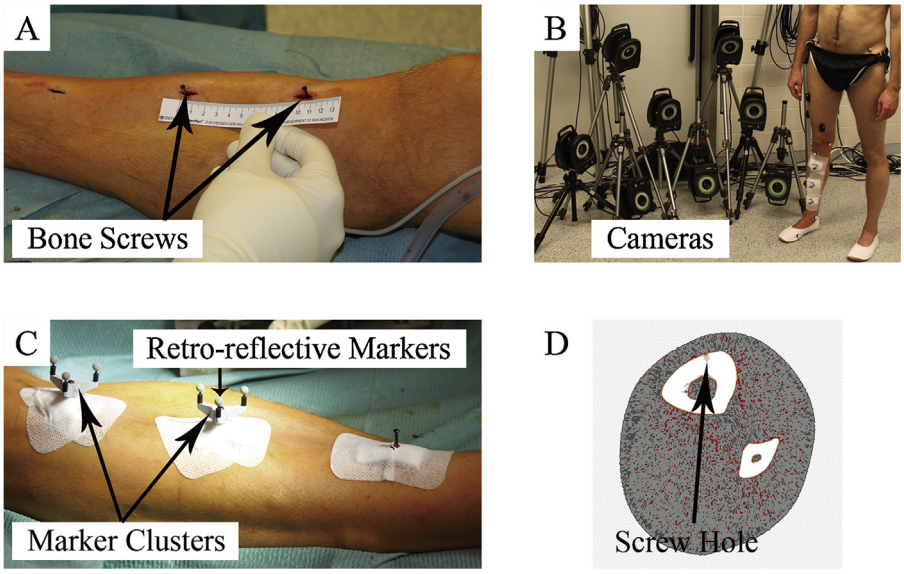


**Fig. 1.** Illustration of the surgical technique and the OST approach in this study. (A) Bone screw implantation into the tibia cortex. (B) The motion capture system with 8 high resolution cameras to track the retro-reflective markers. (C) Marker clusters were fixed on the top of the bone screws. (D) The pQCT image of the cross section area of the shank. The black arrow indicates the screw hole after the bone screw being removed.

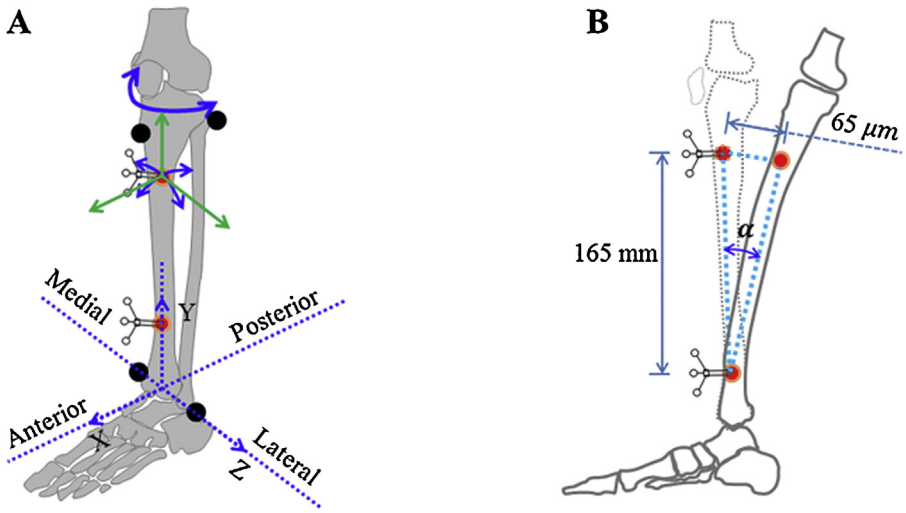


**Fig. 2.** Sketch of the relative position between proximal and distal marker clusters. (A) The movement of proximal marker clusters with respect to the distal one, including three Cardan angles (solid blue arrow) and three translations (solid green arrow). Dashed arrows: Shank Anatomical Coordinate System (SACS); Black spot: the location of the skin attached markers used to determine the SACS. (B) Posterior translation with 65 μm of the proximal marker cluster with respect to the distal one. $\alpha$ was the posterior bending angle induced by posterior translation. (For interpretation of the references to color in this figure legend, the reader is referred to the web version of the article.)

and jumping, was evaluated. More specifically, between the repetitions of the exercises, the trajectories of the tibia-affixed markers were captured at 300 Hz for 1–2 s while the subjects were static in the sitting position and the shank was free of any loading. To label the orientation of the shank in 3D, skin-attached retro-reflective markers (⌀16 mm, Vicon Motion System Ltd., LA, USA) at the position of shank anatomical landmarks (black spots in Fig. 2A), meaning the tip of medial and lateral malleolus, tip of tibia tuberosity and the head of fibula, were captured for further generating Shank Anatomical Coordinate System (SACS) [11]. More specifically, the origin of the SACS was located at the midpoint of the line between the medial and lateral malleolus. Positive *X*, *Y* and *Z* axis referred to anterior, upwards and lateral aspects, respectively.

### 2.5. Reliability assessment: tibia deformation during squatting

Tibia-affixed marker trajectories were captured at 300 Hz, whilst the test subjects were performing squatting with body weight, 20 kg extra weight and 40 kg extra weight, respectively. Prior to the *in vivo* experiments, all test subjects underwent preparatory squatting training twice with different weights on different days to be fully acquainted with the protocol. During the preparatory training, bone screws were installed into a shin pad above the shank instead of into the bone. All squats were performed with the rhythm of 3 s knee bending to maximum knee flexion angles at approximately 90° and 3 s from knee bending returning to standing position. Three to four repetitions were performed at each weight condition. The sampling rate of the system could be conveniently set in the software without changing the hardware configurations. Suitable calibration speed was adopted during the system calibration to work with the marker moving speed during squatting.

### 2.6. Data analysis

The raw trajectory data of the markers was further processed with custom-written routine in MATLAB (The MathWorks, Inc. Version 7.9.0 R2009b).

#### 2.6.1. Resonance frequency analysis

Raw marker trajectories after the flipping impact were Fourier-transformed to compute the frequency spectrum. The modal frequencies, *i.e.* the frequencies with greatest amplitude were taken as the resonance frequencies of the screw-cluster complex.

#### 2.6.2. Determination of the SACS and assessment of the relative movement between tibia-affixed markers clusters across the exercises

For each subject, one frame of the static recording trial was utilized for determining an initial Cartesian SACS from the skin-attached landmarks [11]. The coordinates of the tibia-affixed markers in the SACS were then calculated by coordinate transformation [12,13]. The relative position between every two marker clusters in the SACS were then calculated and expressed as mean ± standard deviation (SD) of three Cardan angles around the axes and three translations along the axis of the SACS, respectively (Fig. 2A).

#### 2.6.3. Assessment of tibia deformation during squatting

The relative movement between the screw-inserted bone sites, which were determined by the marker clusters, was then derived by coordinate transformation in the SACS. During squatting, the relative movement between three bone sites in the SACS was expressed as mean ± standard deviation (SD) of three Cardan angles, *i.e.* internal-external torsion angle, antero-posterior (AP) and medio-lateral (ML) bending angles of entire tibia, upper tibia and lower tibia. In this paper, the peak to peak (p2p) bending and torsion angles of the entire tibia during the squatting cycles are presented. The p2p tibia deformation angles were normalized by dividing the actual distance between the marker clusters for each subject and expressed as degree/meter. The raw deformation angles of entire tibia, upper tibia and lower tibia can be found in the supplementary material.

### 2.7. Statistics

Statistical analyses were performed using the R environment (version 2.15.1, R Development Core Team, 2012). For each subject, the homogeneity variance of the relative position between three marker clusters (three Cardan angles and three translations along the axis of SACS) was tested with the Fligner–Killeen's test. A linear mixed-effects model (the fixed factor: exercise, the random factor: subject) was employed to examine the effects of exercises on the changes of the relative position between marker clusters. A one-way ANOVA linear model was employed to examine the main

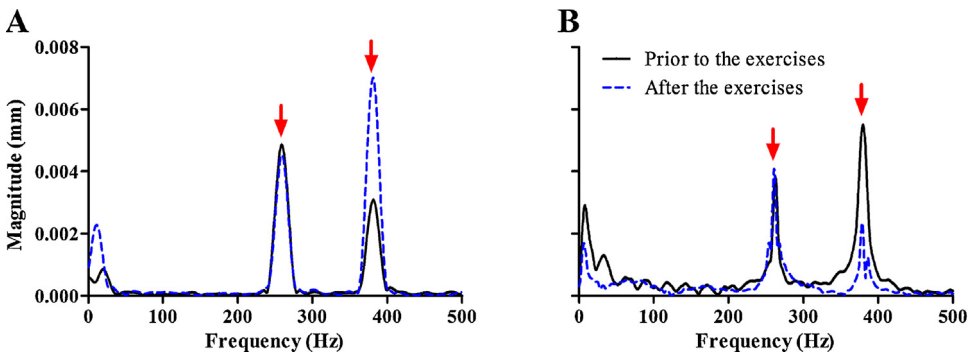


**Fig. 3.** Frequency spectrum of the marker trajectories after the structure of bone screw and marker cluster being flipped by a finger. A and B indicating the results from subject D and E, respectively. Solid black line: Frequency spectrum of the markers recorded prior to all of the exercises; Dashed blue line: Frequency spectrum of the markers recorded after the exercises. Red arrows: the resonance frequencies of the screw-marker structure were approximately 260 Hz and 380 Hz, respectively. (For interpretation of the references to color in this figure legend, the reader is referred to the web version of the article.)

effects of test subject and bearing weight on the tibia deformation angles during squatting. Statistical significance was accepted at $p \leq 0.05$.

## 3. Results

No pain or other issues were reported by the subjects throughout the experiments. At the time of bone screws extraction, all of the bone screws were still firmly inserted into the tibia. No loosening has been observed.

### 3.1. Resonance frequency of the screw-marker structure

There were two vibration modes of the screw-marker structure for each test subject (Fig. 3). The fundamental frequencies were 259 Hz and 262 Hz for two subjects, respectively. The overtone frequencies were 381 Hz and 382 Hz for two subjects, respectively. The resonance frequency of the screw-marker structure did not change after the exercises (Fig. 3, dashed blue curves) comparing that prior to the exercises (Fig. 3, solid black curves).

### 3.2. The relative position of the tibia-affixed markers

For all test subjects, no significant effects of exercises on the homogeneity of the variances of the relative position between every two marker clusters were found ($p = 0.09$). Similarly, from the mixed-effects model, the Cardan angles around $x$ ($p = 0.81$), $y$ ($p = 0.73$), $z$ axis ($p = 0.46$) and the translations along $x$ ($p = 0.09$), $y$ ($p = 0.50$), $z$ axis ($p = 0.14$) were comparable before and after the exercises (minimum $p = 0.09$).

The mean and SD of the relative position between clusters before and after the hopping and jumping tasks from one subject has been summarized in Table 1 as an example. After hopping and jumping, the largest change of the Cardan angle between marker clusters was from $0.19^\circ \pm 0.02^\circ$ to $0.22^\circ \pm 0.02^\circ$ (Cardan angle around $Z$ axis between the distal marker cluster and the middle one). The largest change in translation was found from $-1.210 \pm 0.058$ mm to $-1.143 \pm 0.045$ mm in the $X$ axis between the proximal and middle marker clusters. Among the repetitions of the same task, the largest variation (SD) of the Cardan angle and translation were 0.06° and 65 μm, respectively.

### 3.3. Normalized tibia deformation angles during the squatting exercise

During squats, the proximal tibia bent to its posterior aspect, lateral aspect and twisted to the external aspect with respect to the distal tibia. The deformation results (Fig. 4) are presented on the basis of the individual subject due to the significant main effects of subject on the bending angle ($p < 0.001$) and torsion angle ($p < 0.001$). The AP bending deformation increased with the squat weight for all test subjects ($p < 0.001$). Larger ML bending ($p < 0.001$) and torsion deformation ($p = 0.008$) were found during squats with 40 kg extra weight than 20 kg. The standard deviation for AP (between 0.08°/m and 0.38°/m), ML bending deformation (between 0.04°/m and 0.47°/m) and torsion deformation (between 0.09°/m and 0.65°/m) remained small during the repetitions of squats.

## 4. Discussion and conclusions

To summarize, an OST approach for assessing *in vivo* long bone segment deformation regimes has been applied in an *in vivo* study in humans for the first time. In this study, the feasibility

**Table 1**
The relative position between pairs of marker clusters in SACS.

| Marker clusters | Tasks | Cardan angle (Degree) | | | Translations (mm) | | |
|---|---|---|---|---|---|---|---|
| | | *x* axis | *y* axis | *z* axis | *x* axis | *y* axis | *z* axis |
| Prox. *vs.* Distal | Hopping | 0.07 ± 0.01 | −0.01 ± 0.02 | −0.09 ± 0.01 | 12.688 ± 0.065 | 207.462 ± 0.010 | −0.300 ± 0.031 |
| | Jumping | 0.09 ± 0.02 | −0.01 ± 0.01 | −0.10 ± 0.01 | 12.649 ± 0.043 | 207.473 ± 0.012 | −0.285 ± 0.028 |
| Prox. *vs.* Mid. | Hopping | −0.04 ± 0.02 | −0.04 ± 0.02 | 0.11 ± 0.02 | 1.210 ± 0.058 | 107.712 ± 0.005 | 0.515 ± 0.035 |
| | Jumping | −0.04 ± 0.03 | −0.03 ± 0.06 | 0.12 ± 0.02 | 1.143 ± 0.045 | 107.716 ± 0.006 | 0.488 ± 0.018 |
| Distal *vs.* Mid. | Hopping | −0.11 ± 0.02 | −0.03 ± 0.01 | 0.19 ± 0.02 | −10.774 ± 0.050 | −99.793 ± 0.010 | 1.221 ± 0.030 |
| | Jumping | −0.13 ± 0.02 | −0.05 ± 0.03 | 0.22 ± 0.02 | −10.718 ± 0.035 | −99.805 ± 0.020 | 1.250 ± 0.024 |

For all of the repeated static trials between hopping and jumping, the mean and standard deviation of the relative position between marker clusters were determined. Prox. *vs.* Distal: the position of proximal marker cluster with respect to the distal marker cluster in SACS; Prox. *vs.* Mid.: the position of proximal marker cluster with respect to the middle marker cluster in SACS; Distal *vs.* Mid.: the position of distal marker cluster with respect to the middle marker cluster in SACS. SACS: shank anatomical coordinate system.

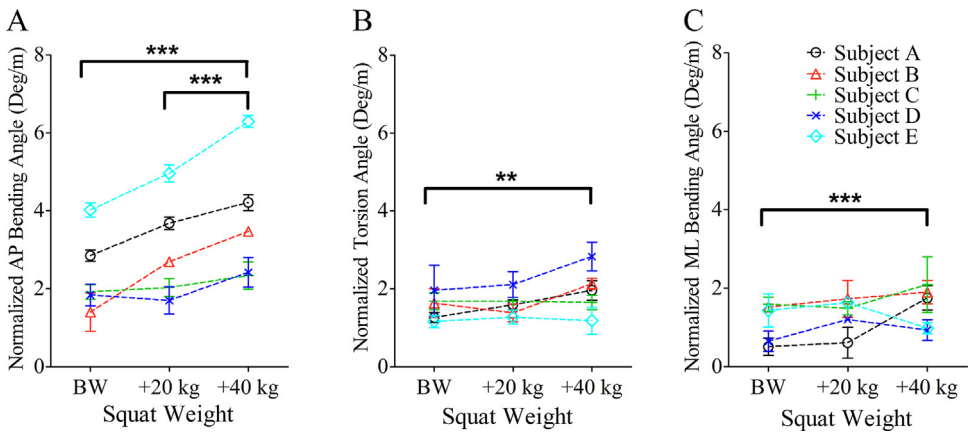


**Fig. 4.** Normalized tibia deformation angles during squats with different weight. The p2p tibia deformation angles were normalized by dividing the actual distance between the marker clusters for each subject and expressed as Degree/meter. (A) Normalized tibia AP bending angles; (B) normalized tibia torsion angle; and (C) normalized tibia ML bending angle. ** $p < 0.01$; *** $p < 0.001$.

of the OST approach has been demonstrated in terms of general toleration, cluster stability and resonance frequency, and deformation reliability during repeated squats cycles. Results suggested that the resonance frequency remain unchanged after the exercises, implying that the bone screws were firmly implanted into the tibia cortex across the intense exercises. Furthermore, the influences of the intense exercises on the relative positions of the tibia-affixed markers remained in a low level, even though the sample size was limited in the present study (minimum $p = 0.09$ for five subjects). The variability of the recorded normalized tibia deformation angles (standard deviation) between the squats repetitions remained relatively small, typically in the range 0.04°/m–0.65°/m.

### 4.1. Pain assessment

Considering the invasive nature of the OST approach, pain induced by the surgical procedure and bone screw insertion has been assessed previously using pain questionnaire, *i.e.* from 0 to 10 indicating pain free to intolerable pain [10]. The pain rating results suggested that pain is not an issue throughout the exercises [10] and is unlikely to influence the *in vivo* experiments.

### 4.2. Stability of bone screws in the tibia cortex and tibia deformation during squats

Resonance frequency analysis is a well-developed approach to assess the stability of the fixation method, *e.g.* during the stability analysis of implants *in vivo* [14,15]. The present near constant resonance frequencies of the screw-marker structure after the exercises, as well as the clear frequency modes obtained in the spectra, indicate that bone screws were tight and did not loosen during the highly intensive activities. Considering that the resonance frequency of the tibia is approximately 110 Hz [16,17] and the frequency component of the ground reaction force (GRF) during hopping was less than 20 Hz (Supplementary material), common sense suggests that potential contributions of the GRF and tibia vibration to the resonance vibration of the screw-cluster structure are irrelevant.

The relative displacement between the tibia-affixed markers prior to and after the intense exercises would be an ideal indicator of the bone screw stability, since the displacement between the markers would not be repeatable if the pins loosen. The largest variance of Cardan angle, *i.e.* 0.06°, and translations induced bending angle, *i.e.* 0.02°, (see Fig. 2B and related calculations in the supplementary material) suggests that any deformation angle change above 0.06° could be detected. The high detection limit indicates a firm installation of the screw-cluster structure in the tibia cortex across all exercises, which provides the crucial requirement for the *in vivo* application of the OST approach. Hence, it can be concluded that the slight changes of the relative position between the markers were not induced by screw loosening, but might mainly have contributed by the recording noise of the motion capture system [9,18–21].

Furthermore, the small variability of the tibia normalized deformation angle (0.04°/m–0.65°/m) between the repetitions of squats indicated high repeatability of the OST approach during tibia deformation measurements and good reliability of the OST approach in *in vivo* tibia deformation recording.

### 4.3. Advantages and limitations

Several benefits can be expected from the OST approach. Firstly, compared to the traditional strain gauge methods, the OST approach needs smaller incisions and either no further bone surface preparations. Secondly, integrating the GRF with the present kinematic results, kinetics analysis may be performed to compute the tibia internal loading. This could be clinically relevant, *e.g.* in the research on stress fractures. Thirdly and most importantly, the quality of the recorded data with the OST approach can be evaluated by assessing the stability of the fixation of clusters as presented in this paper. All these are advantages of OST over traditional strain gauge approaches.

On the other hand, some open questions are left. Firstly, in line with the other *in vivo* bone strain recording approaches, the invasiveness might still be one of the obstacles to expand the OST approach to further research fields. Secondly, further verification of the OST approach with alternative approaches, *e.g.* the promising, non-invasive computer modeling [22,23], linear variable differential transformer or digital imaging approaches [24,25], would be very helpful for expanding the application. Thirdly, like all the current available *in situ* measuring techniques, the sites or bones the OST approach can be applied to are limited due to the interference of the adjacent muscle tissue. Fourthly, the OST approach could not provide local strain levels directly, but only presents tibia segment deformations. Integrating the present results with a Finite Element model of bone would be very promising to derive strain distribution across the bone shaft in future studies. Fifthly, although the sampling rate of the OST approach can be dynamically adjusted as required below 370 Hz without losing resolution, in the present study, the sampling rate is set at 300 Hz due to the demand of a certain capture volume and relatively fast movement capturing.

Possible high resonance vibrations of the screw-cluster structure during intense dynamic exercises may be impossible to be captured, thus leading to the aliasing issue. Although this was unlikely to happen during squatting, the ideal solution to avoid this problem is to sample the signal with a higher sampling rate. Sixthly, the limited sample size in the present study may lose the power to interpret the resonance frequency results and the statistic results. An advanced optical system and a larger sample size would be appreciated for future studies.

### 4.4. Conclusions

Taking together these results, we conclude that the OST approach is feasible and well tolerated, that screw fixation is stable in our study, that measurements of bone deformation are unlikely to be affected by resonance problems and that the *in vivo* assessment of tibia loading pattern in terms of tibia segment deformation recording is reliable. It is very perceivable that the new OST approach lends itself to more ample application wherever insights into bone function are desired. This may cover quite a large field, ranging from biomechanical studies into specific exercises, and quite as much into clinical studies on fractures or osteoporotic patients.

## Funding

None.

## Ethical approval

This study was approved by the relevant ethics bodies, namely the ethical committee of the North-Rhine Medical Board in Düsseldorf (reference number: 2011306) and the ethical committee of the Faculty of Medicine in the University of Cologne (reference number: 12-007).

## Acknowledgments

We would like to thank Hans-Martin Küsel-Feldker and Jürgen Geiermannat the Institute of Biomechanics and Orthopaedics, German Sport University Cologne, for fine manufacturing the marker clusters. Thanks to Andreas Kriechbaumer and Peter Gauger for their kind help during the data collection. Peng-Fei Yang acknowledges his scholarship by the China Scholarship Council (CSC No.: 2009629013).

## Appendix A. Supplementary data

Supplementary data associated with this article can be found, in the online version, at http://dx.doi.org/10.1016/j.medengphy.2014.05.005.

## Conflict of interests

None declared.

## References

[1] Robling AG, Hinant FM, Burr DB, Turner CH. Improved bone structure and strength after long-term mechanical loading is greatest if loading is separated into short bouts. J Bone Miner Res 2002;17:1545–54.
[2] Frost HM. Wolff's law and bone's structural adaptations to mechanical usage: an overview for clinicians. Angle Orthod 1994;64:175–88.
[3] Ruff C, Holt B, Trinkaus E. Who's afraid of the big bad Wolff?: "Wolff's law" and bone functional adaptation. Am J Phys Anthropol 2006;129:484–98.
[4] Turner CH. Three rules for bone adaptation to mechanical stimuli. Bone 1998;23:399–407.
[5] Biewener AA, Thomason JJ, Lanyon LE. Mechanics of locomotion and jumping in the horse (Equus): in vivo stress in the tibia and metatarsus. J Zool 1988;214:547–65.
[6] Rubin CT, Lanyon LE. Limb mechanics as a function of speed and gait – a study of functional strains in the radius and tibia of horse and dog. J Exp Biol 1982;101:187–211.
[7] Lieberman DE, Polk JD, Demes B. Predicting long bone loading from cross-sectional geometry. Am J Phys Anthropol 2004;123:156–71.
[8] Yang PF, Bruggemann GP, Rittweger J. What do we currently know from in vivo bone strain measurements in humans. J Musculoskelet Neuronal Interact 2011;11:8–20.
[9] Yang PF, Sanno M, Bruggemann GP, Rittweger J. Evaluation of the performance of a motion capture system for small displacement recording and a discussion for its application potential in bone deformation in vivo measurements. Proc Inst Mech Eng H 2012;226:838–47.
[10] Ganse B, Yang PF, Brüggemann GP, Müller LP, Rittweger J, Koy T. In vivo measurements of human bone deformation using optical segment tracking: surgical approach and validation in a three-point bending test. J Musculoskelet Neuronal Interact 2014;14:95–103.
[11] Grood ES, Suntay WJ. A joint coordinate system for the clinical description of three-dimensional motions: application to the knee. J Biomech Eng 1983;105:136–44.
[12] Lafortune MA, Cavanagh PR, Sommer 3rd HJ, Kalenak A. Three-dimensional kinematics of the human knee during walking. J Biomech 1992;25:347–57.
[13] Söderkvist I, Wedin P-Å. Determining the movements of the skeleton using well-configured markers. J Biomech 1993;26:1473–7.
[14] Isaacson BM, Vance RE, Chou TG, Bloebaum RD, Bachus KN, Webster JB. Effectiveness of resonance frequency in predicting orthopedic implant strength and stability in an in vitro osseointegration model. J Rehabil Res Dev 2009;46:1109–20.
[15] Meredith N, Book K, Friberg B, Jemt T, Sennerby L. Resonance frequency measurements of implant stability in vivo. A cross-sectional and longitudinal study of resonance frequency measurements on implants in the edentulous and partially dentate maxilla. Clin Oral Implants Res 1997;8:226–33.
[16] Collier RJ, Donarski RJ. Non-invasive method of measuring resonant frequency of a human tibia in vivo part 1. J Biomed Eng 1987;9:321–8.
[17] Collier RJ, Donarski RJ. Non-invasive method of measuring the resonant frequency of a human tibia in vivo part 2. J Biomed Eng 1987;9:329–31.
[18] Gopfert B, Krol Z, Freslier M, Krieg A. 3D video-based deformation measurement of the pelvis bone under dynamic cyclic loading. Biomed Eng Online 2011;10:60.
[19] Liu H, Holt C, Evans S. Accuracy and repeatability of an optical motion analysis system for measuring small deformations of biological tissues. J Biomech 2007;40:210–4.
[20] Schmidt J, Berg DR, Ploeg H-L. Precision, repeatability and accuracy of Optotrak optical motion tracking systems. Int J Exp Comput Biomech 2009;1:114–27.
[21] Windolf M, Gotzen N, Morlock M. Systematic accuracy and precision analysis of video motion capturing systems – exemplified on the Vicon-460 system. J Biomech 2008;41:2776–80.
[22] Al Nazer R, Klodowski A, Rantalainen T, Heinonen A, Sievanen H, Mikkola A. A full body musculoskeletal model based on flexible multibody simulation approach utilised in bone strain analysis during human locomotion. Comput Methods Biomech Biomed Eng 2011;14:573–9.
[23] Al Nazer R, Rantalainen T, Heinonen A, Sievanen H, Mikkola A. Flexible multibody simulation approach in the analysis of tibial strain during walking. J Biomech 2008;41:1036–43.
[24] Grecula MJ, Morris RP, Laughlin JC, Buford Jr WL, Patterson RM. Femoral surface strain in intact composite femurs: a custom computer analysis of the photoelastic coating technique. IEEE Trans Biomed Eng 2000;47:926–33.
[25] Yang L, Zhang P, Liu S, Samala PR, Su M, Yokota H. Measurement of strain distributions in mouse femora with 3D-digital speckle pattern interferometry. Opt Laser Eng 2007;45:843–51.